SUGISAKA MASANORI

Journal of Robotics, Networking and Artificial Life
Vol. 9(2); September (2022), pp. 128–135
ISSN (Online):2352-6386; ISSN (Print):2405-9021
https://alife-robotics.org/jrnal.html

Research Article

A MBD-based Knee Link Model to Analyze Singular Postures to Find Necessary Restrictions Toward Personalized Knee Support Exoskeleton

Shintaro Kasai[1], Pancho Dachkinov[1], Kohei Tanaka[1], Hiroaki Wagatsuma[1,2]
[1]*Kyushu Institute of Technology, 4 Hibikino, Wakamatsu-ku, Kitakyushu, 808-0196, Japan*
[2]*RIKEN CBS, Japan*

ARTICLE INFO

Article History

Received 25 November 2021
Accepted 24 March 2022

Keywords

Knee support
Exoskeleton-type assistive device
Multi-body dynamics (MBD)
Joint dysfunction

ABSTRACT

Assistive devices have been studied in the senses of the universal design and a possible simplification for mass production, and such a concept can be extended to the personalization by using advanced 3D printing technologies, which allows to provide suitable exoskeleton-type devices to fit for the subject's body to achieve symptom relief. A systematic analytical mechanics is highly important for the investigation of proposed integrative systems and multibody dynamics and its computer simulation enhance the capability to find potential problems in design, for example risky postures for the subject. We introduced multibody dynamics to analyze a knee support exoskeleton by using a linkage system newly designed as a simplification of the device. In the computer experiment, a singular posture was successfully found as the limitation of the device to move safely for subjects having joint dysfunctions.

1. Introduction

In the ambulatory function, knee joints bear the body weight and then it is vulnerable especially in elderly persons. Problems in joints, or knee injuries, impact on their abilities in daily life [1]. Therefore, a biomechanical analysis to compare normal and injured conditions in the knee joint function is necessary for finding potential problems and possible supports by assistive devices. In other words, the introduction of theoretical and computerized design methods for knee assistive devices has a large potential for parameter optimizations of the device's specification for sake of making a successful rehabilitation program. Assistive devices to attach the human body known as exoskeletons have been provided in the stage of the convalescence stage of the rehabilitation or the prevention of serious motor dysfunctions. The devices have developed in recent years by using motorized mechanisms and spring-damper parts [2,3]. If joints in the human body were modeled as a simple rotational joint to be able to replace by rotational actuators, pendulum models can be considered to enhance walking functions in normal and fast gaits [2,4]. On the other hand, it is still unclear to define best parameters to realize a dynamic adaptation to motion kinetics in actual walking environments. Then model-based kinematic and kinetic analyses are highly important for the clarification of specifications such as joint torque and knee stiffness [4,5]. The systematic analysis can extend future capabilities of exoskeleton-type assistive devices and contribute the assurance of quality [6,7,8].

In the present study, we studied a systematic theoretical analysis based on the multibody dynamics (MBD)

Corresponding author's E-mail: kasai.shintaro660@mail.kyutech.jp, dachkinov.pancho-nikolaev608@mail.kyutech.jp, tanaka.kohei886@mail.kyutech.jp, waga@brain.kyutech.ac.jp https://www.kyutech.ac.jp/

[9,10,11,12,13] applied to the proposed knee mechanism in the aim of motion kinetics analysis toward the knee joint support. The systematic analytical method based on MBD clarifies joint torque and knee stiffness in the target motion, which helps in the investigation of supportive mechanisms for a load reduction of the joint. The model-based analysis provides detail inspection for timing and position analyses to be able to improve support devices.

2. Methodology

2.1. Knee link model

Human knee joints are organized internally with two ligaments to form a four-bar linkage mechanism as discussed by Shenoy et al. [14] (Fig. 1). It is called a roll-back mechanism because the center of the upper rotational point (black circle in Fig. 1) shifts back during the bending motion when the knee straight posture changes to knee bent postures. The mechanism cannot be replaced by a simple rotary joint. Such a complex biomechanism is not easily reproduced and supported in the form of the exoskeleton-type device, while welfare device expert designers reproduce a suitable device based on their knowledge and experiences. Fig. 2 is a proto-type of the knee support device to attempt to reproduce the roll-back mechanism by the combination of rotational joints and translational movements [15]. However, the effectiveness of the design need to be clarified not only in the posture analysis but also the force estimation at each rotational parts in the device. This is important for further theoretical optimization to pursue what is the best structure.

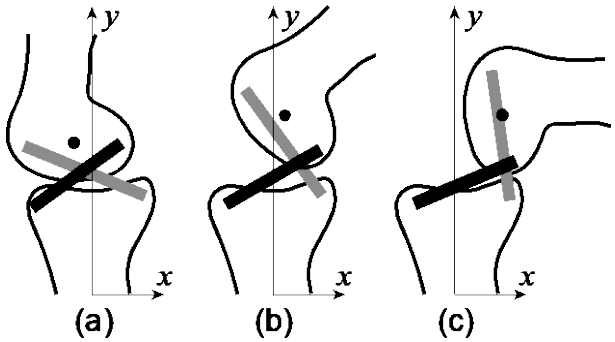

Fig. 1. A schematic illustration of the biomechanics of the knee joint [14]. Upper and lower bodies in the joint are bound with the posterior cruciate ligament (PCL, represented by the gray bar) and the anterior cruciate ligament (ACL, the black bar).

Fig. 2. A prototype exoskeleton-type knee joint support device [15].

2.2. *MBD for knee link model*

In consideration of linkage motions with angler change in individual joints, a constant angular velocity can be given to the joint p3 (Fig. 1 (b)) to mimic the knee joint extension, which was analyzed in the multibody dynamics (MBD) [9,10,11,12,13]. By using MBD, the numerical analysis provides the posture and force analyses by describing the motion equation in an algebraic way to represent the structural system with various components. The differential equations are described in the form of the matrix with given constraints, and the actual solution is derived from the numerical integration method in the computer experiment. In MBD, the differential algebraic equation is reconstructed based on generalized coordinates, which are provided from transformations of local coordinates in individual components. As the forward dynamics analysis, the differential algebraic equation as shown in Eq. (1) is initially formed to represent the target system. The meanings of the characters in Eq. (1) are as Table 1.

Individual positions of bodies of the system and velocities, acceleration and other factors are obtained in the analysis.

$$\begin{bmatrix} M & \Phi_q^T \\ \Phi_q & 0 \end{bmatrix} \begin{bmatrix} \ddot{q} \\ \lambda \end{bmatrix} = \begin{bmatrix} Q^A \\ \gamma \end{bmatrix} \tag{1}$$

Table 1. The planning and control components.

M	Mass matrix
Φ_q	Jacobian matrix differentiated from constraint equation in generalized coordinates
$\ddot{q}$	Generalized acceleration matrix
λ	Lagrange multiplier
Q^A	Generalized force
γ	Acceleration equation

Fig. 3 shows the angle and the mass-center coordinates of each link and Table 2 shows the lengths of each link. The following equations express the generalized coordinate matrix and the generalized velocity matrix for each mass center.

$$q_i = \begin{bmatrix} x_i & y_i & \theta_i \end{bmatrix}^T \tag{2}$$

$$\dot{q}_i = \begin{bmatrix} \dot{x}_i & \dot{y}_i & \dot{\theta}_i \end{bmatrix}^T \tag{3}$$

The generalized coordinate matrix and the generalized velocity matrix were derived as follows.

$$q_i = \begin{bmatrix} q_1 & q_2 & q_3 & q_4 & q_5 & q_6 \end{bmatrix}^T \tag{4}$$

$$\dot{q}_i = \begin{bmatrix} \dot{q}_1 & \dot{q}_2 & \dot{q}_3 & \dot{q}_4 & \dot{q}_5 & \dot{q}_6 \end{bmatrix}^T \tag{5}$$

Table 2: Parameters in the link model

Link name	Sides	Length [mm]
*L*1	O-r1	82
*L*2	r1-r2	47
*L*3	r2-r4	37
*L*4	r3-d	190
*L*5	r3-r4	14
*L*6	r1-r3	80

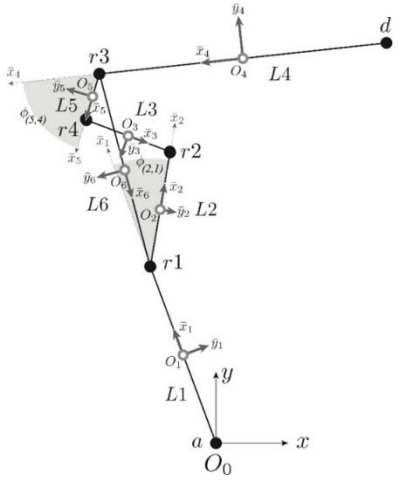

Fig. 3. The definition of generalized coordinates.

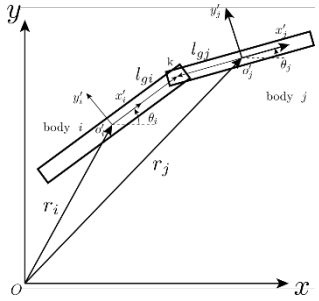

Fig. 4. The definition of kinematic constraints of rotary joint.

For describing the connections and movements of each link in the knee link model, the definitions of the constraints of each link and joint were needed. The kinematic constraints of rotary joints in the general multi body systems were defined as shown in Fig. 4 and represented as follows.

$$\begin{aligned} \Phi^K_{R(i,j)} &= \left(\begin{bmatrix} x_j \\ y_j \end{bmatrix} + A_j \begin{bmatrix} -l_{gj} \\ 0 \end{bmatrix} \right) - \left(\begin{bmatrix} x_i \\ y_i \end{bmatrix} + A_i \begin{bmatrix} l_{gi} \\ 0 \end{bmatrix} \right) \\ &= \begin{bmatrix} x_j - x_i - lgj\cos\theta_j - lgi\cos\theta_i \\ y_j - y_i - lgj\sin\theta_j - lgi\sin\theta_i \end{bmatrix} = 0 \end{aligned} \tag{6}$$

In the expanded form, the kinematic constraints in the system finally represented as follows.

$$\Phi^K = \begin{bmatrix} \Phi^K_{R12} \\ \Phi^K_{R23} \\ \Phi^K_{R35} \\ \Phi^K_{R54} \\ \Phi^K_{R16} \\ \Phi^K_{R64} \end{bmatrix}$$

$$= \begin{bmatrix} \left(\begin{bmatrix} x_2 \\ y_2 \end{bmatrix} + A_2 * \begin{bmatrix} -l_2/2 \\ 0 \end{bmatrix} \right) - \left(\begin{bmatrix} x_1 \\ y_1 \end{bmatrix} + A_1 * \begin{bmatrix} l_1/2 \\ 0 \end{bmatrix} \right) \\ \left(\begin{bmatrix} x_3 \\ y_3 \end{bmatrix} + A_3 * \begin{bmatrix} l_3/2 \\ 0 \end{bmatrix} \right) - \left(\begin{bmatrix} x_2 \\ y_2 \end{bmatrix} + A_2 * \begin{bmatrix} l_2/2 \\ 0 \end{bmatrix} \right) \\ \left(\begin{bmatrix} x_5 \\ y_5 \end{bmatrix} + A_5 * \begin{bmatrix} l_5/2 \\ 0 \end{bmatrix} \right) - \left(\begin{bmatrix} x_3 \\ y_3 \end{bmatrix} + A_3 * \begin{bmatrix} -l_3/2 \\ 0 \end{bmatrix} \right) \\ \left(\begin{bmatrix} x_4 \\ y_4 \end{bmatrix} + A_4 * \begin{bmatrix} l_4/2 \\ 0 \end{bmatrix} \right) - \left(\begin{bmatrix} x_5 \\ y_5 \end{bmatrix} + A_5 * \begin{bmatrix} -l_5/2 \\ 0 \end{bmatrix} \right) \\ \left(\begin{bmatrix} x_6 \\ y_6 \end{bmatrix} + A_6 * \begin{bmatrix} l_6/2 \\ 0 \end{bmatrix} \right) - \left(\begin{bmatrix} x_1 \\ y_1 \end{bmatrix} + A_1 * \begin{bmatrix} l_1/2 \\ 0 \end{bmatrix} \right) \\ \left(\begin{bmatrix} x_4 \\ y_4 \end{bmatrix} + A_4 * \begin{bmatrix} l_4/2 \\ 0 \end{bmatrix} \right) - \left(\begin{bmatrix} x_6 \\ y_6 \end{bmatrix} + A_6 * \begin{bmatrix} -l_6/2 \\ 0 \end{bmatrix} \right) \end{bmatrix} \quad (7)$$

The link 1 is fixed vertically, and then x_1, y_1 and θ_1 is provided according to the absolute constraints as follows. In absolute constraints, the angle constraints of ϕ_{12}(L1 - L2) and ϕ_{54}(L5 – L4) are also defined.

$$\Phi^A = \begin{pmatrix} x_1 \\ y_1 - L_1 \\ \theta_1 - \frac{\pi}{2} \\ \theta_1 - \theta_2 - \phi_{12} \\ \theta_5 - \theta_4 - \phi_{54} \end{pmatrix} \quad (8)$$

When a constant angular velocity is given in the joint r3, the driving constraints is represented as follows.

$$\Phi^D = \theta_4 - \omega\, t \quad (9)$$

The kinematic, absolute and driving constraints are combined in the matrix as follows.

$$\Phi = \begin{pmatrix} \Phi^K \\ \Phi^A \\ \Phi^D \end{pmatrix} \quad (10)$$

Finally, the Jacobian matrix is calculated as follows.

$$\Phi_q = \begin{bmatrix} \Phi_{q1} & \Phi_{q2} \\ \Phi_{q3} & \Phi_{q4} \end{bmatrix} \quad (11)$$

$$\Phi_{q1} = \begin{bmatrix} -1 & 0 & l_1\sin(\theta_1)/2 & 1 & 0 & l_2\sin(\theta_2)/2 & 0 & 0 & 0 \\ 0 & -1 & -l_1\cos(\theta_1)/2 & 0 & 1 & -l_2\cos(\theta_2)/2 & 0 & 0 & 0 \\ 0 & 0 & 0 & -1 & 0 & l_2\sin(\theta_2)/2 & 1 & 0 & -l_3\sin(\theta_3)/2 \\ 0 & 0 & 0 & 0 & -1 & -l_2\cos(\theta_2)/2 & 0 & 1 & l_3\cos(\theta_3)/2 \\ 0 & 0 & 0 & 0 & 0 & 0 & -1 & 0 & -l_3\sin(\theta_3)/2 \\ 0 & 0 & 0 & 0 & 0 & 0 & 0 & -1 & l_3\cos(\theta_3)/2 \\ 0 & 0 & 0 & 0 & 0 & 0 & 0 & 0 & 0 \\ 0 & 0 & 0 & 0 & 0 & 0 & 0 & 0 & 0 \\ -1 & 0 & l_1\sin(\theta_1)/2 & 0 & 0 & 0 & 0 & 0 & 0 \end{bmatrix} \quad (12)$$

$$\Phi_{q2} = \begin{bmatrix} 0 & 0 & 0 & 0 & 0 & 0 & 0 & 0 & 0 \\ 0 & 0 & 0 & 0 & 0 & 0 & 0 & 0 & 0 \\ 0 & 0 & 0 & 0 & 0 & 0 & 0 & 0 & 0 \\ 0 & 0 & 0 & 0 & 0 & 0 & 0 & 0 & 0 \\ 0 & 0 & 0 & 1 & 0 & -l_5\sin(\theta_5)/2 & 0 & 0 & 0 \\ 0 & 0 & 0 & 0 & 1 & l_5\cos(\theta_5)/2 & 0 & 0 & 0 \\ 1 & 0 & -l_4\sin(\theta_4) & -1 & 0 & l_5\sin(\theta_5)/2 & 0 & 0 & 0 \\ 0 & 1 & l_4\cos(\theta_4) & 0 & -1 & l_5\cos(\theta_5)/2 & 0 & 0 & 0 \\ 0 & 0 & 0 & 0 & 0 & 0 & 1 & 0 & -l_6\sin(\theta_6)/2 \end{bmatrix} \quad (13)$$

$$\Phi_{q3} = \begin{bmatrix} 0 & 1 & l_1\cos(\theta_1)/2 & 0 & 0 & 0 & 0 & 0 & 0 \\ 0 & 0 & 0 & 0 & 0 & 0 & 0 & 0 & 0 \\ 0 & 0 & 0 & 0 & 0 & 0 & 0 & 0 & 0 \\ 1 & 0 & 0 & 0 & 0 & 0 & 0 & 0 & 0 \\ 0 & 1 & 0 & 0 & 0 & 0 & 0 & 0 & 0 \\ 0 & 0 & 1 & 0 & 0 & 0 & 0 & 0 & 0 \\ 0 & 0 & 1 & 0 & 0 & -1 & 0 & 0 & 0 \\ 0 & 0 & 0 & 0 & 0 & 0 & 0 & 0 & 0 \\ 0 & 0 & 0 & 0 & 0 & 0 & 0 & 0 & 0 \end{bmatrix} \quad (14)$$

$$\Phi_{q4} = \begin{bmatrix} 0 & 0 & 0 & 0 & 0 & 0 & 1 & l_6\cos(\theta_6)/2 \\ 1 & 0 & -l_4\sin(\theta_4)/2 & 0 & 0 & 0 & -1 & 0 & -l_6\sin(\theta_6)/2 \\ 0 & 1 & l_4\cos(\theta_4)/2 & 0 & 0 & 0 & 0 & -1 & l_6\cos(\theta_6)/2 \\ 0 & 0 & 0 & 0 & 0 & 0 & 0 & 0 & 0 \\ 0 & 0 & 0 & 0 & 0 & 0 & 0 & 0 & 0 \\ 0 & 0 & 0 & 0 & 0 & 0 & 0 & 0 & 0 \\ 0 & 0 & 0 & 0 & 0 & 0 & 0 & 0 & 0 \\ 0 & 0 & -1 & 0 & 0 & 1 & 0 & 0 & 0 \\ 0 & 0 & 1 & 0 & 0 & 0 & 0 & 0 & 0 \end{bmatrix} \quad (15)$$

In MBD, the Jacobian matrix is used for the differential algebraic equation of the motion equation shown in Eq. (1). The generalized acceleration matrix can numerically be calculated for the detail analysis.

2.3. *Spring-Damper Components*

As the benefit of the MBD-based analysis, any link can be replaced to the spring-damper component and the component bridges between two points as shown in Fig. 5. In this analysis, the spring-damper component was used for the force control system provided by the musculoskeletal system of the human knee joint.

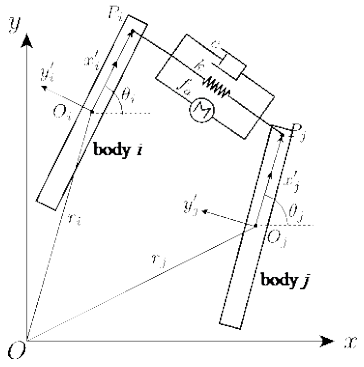

Fig. 5. The definition of the spring-damper (motor) component attached to two points. *c, k* and *fa* respectively denote damping constant, spring constant, and force provided by the implemented actuator.

3. Results

Kinematic and kinetic (dynamics) analysis can be done in the framework of MBD, which are systematically and numerically computed with the differential algebraic equation as described in the previous section. In the knee rigid link model, positions and angles of individual links were derived in the form of generalized coordinates in the numerical analyses by using the Newton-Raphson method and the numerical integration of the Runge-Kutta Gill's method [16] in MATLAB implementations.

The constraint equations such as Eq. (7) can flexibly be modified depending on parts in the system, forces and torques to realize a target motion can be estimated systematically and environmental conditions can be included in the analysis. Therefore, the MBD-based analysis has advantages in 1) the extendibility of parts in the system, 2) driving force estimation by inverse dynamics, 3) variability of external forces.

3.1. *The movement of the knee link model*

In the first place, the movement analysis was demonstrated to test the range of the motion. In the kinematic analysis, the relative angular constraints were given as $\emptyset_{12} = \pi/4$ and $\emptyset_{54} = \pi/4$ and the driving constraint was given as the repetitive vertical movement of the point *d,* which was defined as follows.

$$d_y = 0.5(p^{max} - p^{min}) \cdot \sin(2\pi/T^{unit} \cdot t^{step} + 1) - p^{min} \quad (16)$$

where $p^{max} = 3$, $p^{min} = 2$, $T^{unit} = 2000 \cdot \Delta t$ and $\Delta t = 0.025$ and t^{step} denotes the time step of the computer experiment. Fig. 6 showed the temporal sequence of the behavior of the system in a cycle of $T^{unit} = 50$.

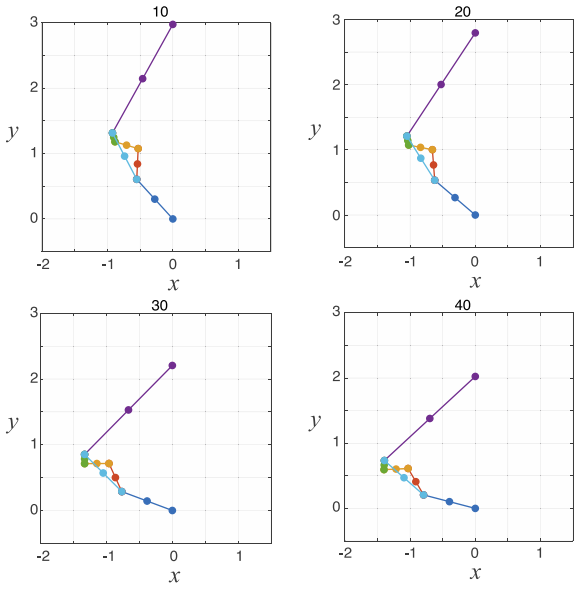

Fig. 6. The MBD-based kinematic analysis of the system.

When a constant angular velocity was given to θ_4 toward bending direction with the knee link extended, the knee link model reproduced the bending motions of knee joint. By the systematic and theoretical analysis, angles, angular velocities and angular accelerations of individual links were clearly analyzed. Giving constant angular velocity to r3, the angle θ_4 was decreasing from $\theta_4 = 90°$. However, when the link angle reaches a certain angle, the rotation of the joint is locked, and then the knee movement is prevented. Interestingly, the result indicated that this knee link model has a limitation of the range of the joint extension in the form of a singular posture (Fig. 7). It happened when link L3 and L5 were aligned in a same straight line. It realized that the rotation of the link is locked at this particular angle and suggest that it is necessary function to prevent the breakage of the knee joint. The original device was designed to embed its limitation with respect to the freedom of the knee joint. In this sense, the result proved the importance of MBD-based singular posture analysis.

The result indicates the limitation of the range of the stretching knee motion, which suggests a necessary knee joint support to prevent the knee joint dysfunction by attaching the assistive device.

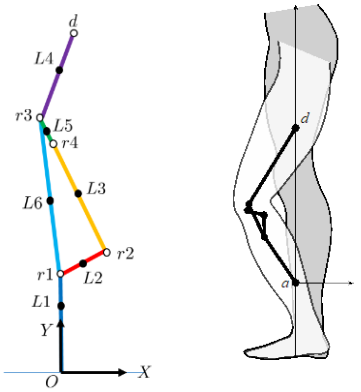

Fig. 7. The singular point posture of the knee model (left). A schematic illustration of the attachment position of the human body (right).

3.2. *The joint load dynamics with spring-damper components*

In the second place, the force analysis was demonstrated in the MBD-based kinetic analysis. As illustrated in Fig. 4 (right), the center of mass of the human body is kept in the straight line to keep the standing posture. It reflects to the kinematic constraint to be the same x position of points a *(O)* and d. Due to the difference from the kinematic analysis to examine possible postures of the linkage, the kinetic analysis based on the set of equations of motion involves mass of all links. As demonstrated in the MBD-based kinetic analysis in Fig. 8, during the driving constraint as well as the previous section by Eq. (16) (different parameters were $T^{unit} = 1000 \cdot \Delta t$ and $\Delta t = 0.0025$ for the observation in the early stage to falling down precisely), the behavior was different from the kinetic analysis and it showed a falling down motion due to its weight. As the dynamics to be physical action of the system without any external force to keep posture, which was clearly demonstrated an actual behavior in the world.

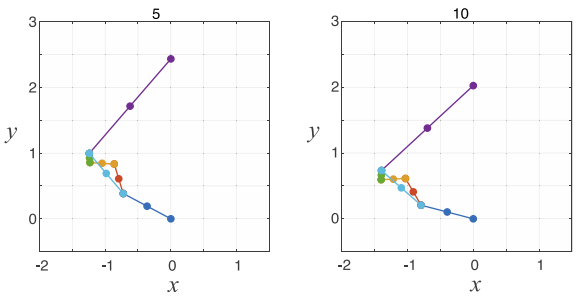

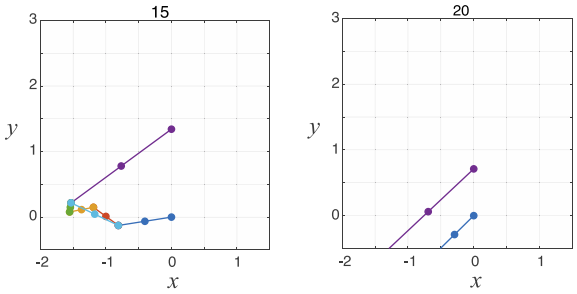

Fig. 8. The MBD-based kinetic (dynamics) analysis of the system without necessary constraints to keep the posture.

Then, a spring-damper mechanism was added to connect between points d and $r1$ as shown in Fig. 9. Parameters were the same as before except $p^{max} = 0.8$, $p^{min} = 0.4388$ for the minimization of the effect from the driving force to observe the effect by the spring-damper system. The external force is generated by the spring damper system as follows.

$$Q_1^e = f_s \begin{bmatrix} 1 & 0 \\ 0 & 1 \\ \left(A_1 V \begin{bmatrix} l_1/2 \\ 0 \end{bmatrix}\right)^T \end{bmatrix} \frac{d_{14}}{|d_{14}|}$$
$$Q_4^e = -f_s \begin{bmatrix} 1 & 0 \\ 0 & 1 \\ \left(A_4 V \begin{bmatrix} -l_4/2 \\ 0 \end{bmatrix}\right)^T \end{bmatrix} \frac{d_{14}}{|d_{14}|} \quad (17)$$

where

$$d_{14} = \begin{bmatrix} d_x \\ d_y \end{bmatrix},$$
$$V = \begin{bmatrix} 0 & -1 \\ 1 & 0 \end{bmatrix}. \quad (18)$$

Therefore, the final form of the external force of Eq. (1) is given as the summation as follows.

$$Q_1^A = \begin{bmatrix} 0 \\ -m_1 g \\ 0 \end{bmatrix} + Q_1^e$$
$$Q_4^A = \begin{bmatrix} 0 \\ -m_4 g \\ 0 \end{bmatrix} + Q_4^e \quad (19)$$

In addition, the parameter of the spring-damper system (Fig. 5) is given as follows.

$$f_s = -k(l - l_0) - c\dot{l} + f_a \quad (20)$$

where $k = 1, l_0 = 1, c = 0.5$ and $f_a = -10$.

3.3. *The results of the kinetic analysis*

After the implementation of the spring-damper system, the temporal evolution in the MBD-based kinetic analysis was demonstrated. Fig. 9 showed the initial stage as a shrinkage behavior and it was recovered according to the spring-damper system (Fig. 10).

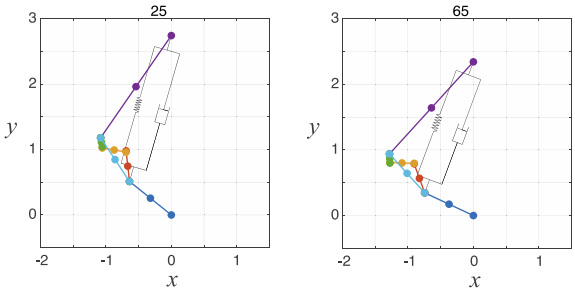

Fig. 9. The initial stage to go down the system due to its weight, which corresponds to the knee flexion.

This result indicates that the MBD-based analysis effective to specify which parts are necessary and what parameters is crucial to achieve the target behavior. In addition, if the force dynamics from the human body and environmental factors can be considered in the combination of force controls, the parts need to be repriced depending to Fig. 7 shows the torque generated in each joint in the bending motion of the link obtained by inverse dynamic analysis. From Fig.7, it is possible to understand the magnitude and timing of the torque generated in each joint. Thus, the proposed linkage model and MBD-based analysis contributed to find a risk in persons with knee joint dysfunction and this timing analysis is important to efficiently support joint movement.

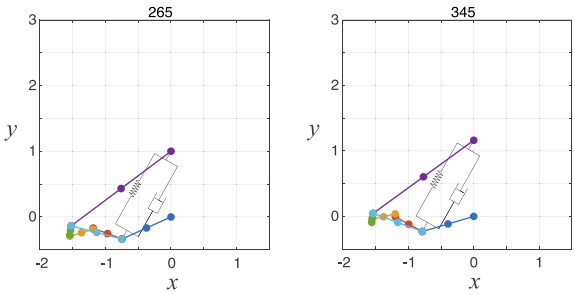

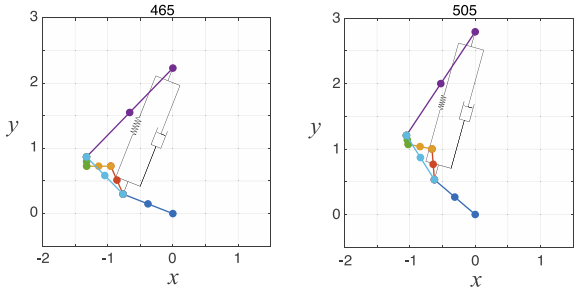

Fig. 10. The recovery stage to push the system up according to the spring-damper-motor system, which corresponds to the knee extension.

4. Conclusion

By using the theoretical background of the MBD analysis and implementation techniques, the knee joint linkage model was examined in the computer experiment. It provided not only the kinematic analysis to find the singular posture, but also force analysis in the kinetic analysis based on the differential algebraic equations in multibody system to represent equations of motion and internal and external constraints. The analysis with the spring-damper system is beneficial for the estimation of the parameter values to realize the target motion. In the present study, we assumed the extension and flexion of the knee joint in the form of the spring-damper system and the fitness of the assistive device will be analyzed in the further extended analysis in the MBD-based analysis. It indicates that the MBD-based analysis is beneficial for the reverse engineering in the process of the support device design to estimate the ideal load reduction at specific knee bending and extension movements. In the further analysis, detail analyses are necessary such as a comparative analysis of models that combines the knee model and various assistive device mechanisms to develop the knee assistive devices.

Acknowledgements

This work was supported in part by JSPS KAKENHI (16H01616, 17H06383), Project on Regional Revitalization Through Advanced Robotics (Kyushu Institute of Technology/Kitakyushu city, Japan) and Kitakyushu Foundation for the Advancement of Industry, Science and Technology (FAIS). The authors gratefully acknowledge ARIZONO orthopedic supplies Co., Ltd. for assistance with the formulation of exoskeleton-type assistive devices in their products.

References

1. L. Zhang, G. Liu, B. Han, Z. Wang, Y. Yan, J. Ma and P. Wei, "Knee Joint Biomechanics in Physiological Conditions and How Pathologies Can Affect It: A Systematic Review," Applied Bionics and Biomechanics, 2020, Article Number 7451683.
2. L. Zhang, Y. Liu, R. Wang, C. Smith and E. Gutierrez-Farewik, "Modeling and Simulation of a Human Knee Exoskeleton's Assistive Strategies and Interaction," Frontiers in Neurorobotics, 2021, 15 620928.
3. W. Wu, J. Fong, V. Crocher, P. Lee, D. Oetomo, Y. Tan and D. Ackland, "Modulation of shoulder muscle and joint function using a powered upper-limb exoskeleton," Journal of Biomechanics, 2018, Apr 27;72:7-16.
4. J. Vantilt, K. Tanghe, M. Afschrift, A. Bruijnes, K. Junius, J. Geeroms, E. Artbelien, F. Groote, D. Lefeber, I. Jonkers and J. Schutter, "Model-based control for exoskeletons with series elastic actuators evaluated on sit-to-stand movements," Journal of Neuroengineering and Rehabilitation, 2019, Jun 3;16(1):65.
5. S. Schrade, Y. Nager, A. Wu, R. Gassert and A. Ijspeert, "Bio-inspired control of joint torque and knee stiffness in a robotic lower limb exoskeleton using a central pattern generator," IEEE, 2017, Jul;2017:1387-1394.
6. R. McGrath, M. Ziegler, M. Pires-Faernandes, B. Knarr, J. Higginson and F. Sergi, "The effect of stride length on lower extremity joint kinematics at various gait speeds," PLoS One, 2019, Feb 22;14(2):e0200862.
7. K. Gui, H. Liu and D. Zhang, "A generalizes framework to achieve coordinated admittance control for multi-joint lower limb robotic exoskeleton," IEEE, 2017, Jul;2017:228-233.
8. K. Mankala, S. Banala and S. Agrawal, "Novel swing-assist um-motorized exoskeletons for gait training," Journal of Neuroengineering and Rehabilitation, 2009, Jul 3;6:24.
9. J. A. C. Ambrósio, Impact of Rigid and Flexible Multibody Systems: Deformation Description and Contact Models, in *Virtual Nonlinear Multibody Systems. NATO ASI Series (Series II: Mathematics, Physics and Chemistry)*, eds. W. Schiehlen and M. Valášek, Springer, Dordrecht, vol 103, 2003, pp. 57-81.
10. P. E. Nikravesh, *Planar Multibody Dynamics: Formulation, Programming with MATLAB, and Applications*, 2nd edn., CRC Press, Boca Raton, 2018.
11. K. Komoda and H. Wagatsuma, Energy-efficacy comparisons and multibody dynamics analyses of legged robots with different closed-loop mechanisms, *Multibody System Dynamics* 40, 2017, pp. 123–153.
12. D. Batbaatar and H. Wagatsuma, A Proposal of the Kinematic Model of the Horse Leg Musculoskeletal System by Using Closed Linkages, *Proceedings of the 2019 IEEE International Conference on Robotics and Biomimetics (ROBIO)*, Dali, China, 2019, pp. 869–874.
13. J. Baumgarte, Stabilization of constraints and integrals of motion in dynamical systems, *Computer Methods in Applied Mechanics and Engineering* 1(1), 1972, pp. 1–16.
14. Arizono orthopedic supplies Co., Ltd.: Products, http://arizono.co.jp/products/products_links/products_2/
15. R. Shenoy, P.S. Pastides, D. Nathwani, (iii) Biomechanics of the knee and TKR, *Orthopaedics and Trauma*, 27(6), 2013, pp. 364-371.
16. Wolfram Research, Inc., Runge-Kutta Gill's method, https://mathworld.wolfram.com/GillsMethod.html

Authors Introduction

Mr. Shintaro Kasai

He received his Bachelor's degree in Engineering in 2021 from the Faculty of Engineering, Kyushu Institute of technology in Japan. He is currently a master student in Kyushu Institute of Technology, Japan

Mr. Pancho Dachkinov

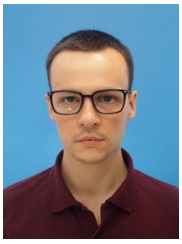

He received his Master's degree in Engineering in 2018 from the Technical University of Sofia, Bulgaria. He worked in the Institute of Robotics – Bulgarian Academy of Sciences 2016-2019. He is currently a doctoral student in Kyushu Institute of Technology, Japan

Mr. Kohei Tanaka

He is currently a fourth grade undergraduate student in Department of Mechanical and Control Engineering, Faculty of Engineering, Kyushu Institute of Technology, Japan. He is interested in 3D printing and compliant mechanisms.

Dr. Hiroaki Wagatsuma

He received his M.S., and Ph.D. degrees from Tokyo Denki University, Japan, in 1997 and 2005, respectively. In 2009, he joined Kyushu Institute of Technology, where he is currently an Associate Professor of the Department of Human Intelli- gence Systems. His research interests include non- linear dynamics and robotics. He is a member of IEEE.